

# Control of Polystyrene Film Dewetting through Sulfonation and Metal Complexation

Yi Feng,<sup>†</sup> Alamgir Karim,<sup>\*,‡</sup> Robert A. Weiss,<sup>\*,†</sup> Jack F. Douglas,<sup>‡</sup> and Charles C. Han<sup>‡</sup>

*Institute of Materials Science, University of Connecticut, Storrs, Connecticut, 06269, and Polymers Division, National Institute of Standards and Technology, Gaithersburg, Maryland 20899*

*Received May 9, 1997; Revised Manuscript Received October 10, 1997*<sup>®</sup>

**ABSTRACT:** The dewetting of low molecular weight sulfonated polystyrene ionomers (SPS) on inorganic silicon oxide substrates is compared with unmodified polystyrene (PS,  $M_w = 4000$ ) using a combination of X-ray reflectivity, optical and atomic force microscopy. The amounts of sulfonate group and metal counterion ( $\text{Li}^+$ ,  $\text{Zn}^{2+}$ ) were both varied in our study. Unlike unmodified PS, which readily dewets the substrate, a strong inhibition of dewetting occurs for low sulfonation ( $\approx 2.3$  mol %), and no apparent dewetting was found for high sulfonation ( $\geq 7$  mol %). For ZnSPS, dewetting was not observed in any of the films, even for those with very low sulfonation. Comparison with bulk rheological data suggests that inter- and intramolecular ionomer complexation may be important in retarding the dewetting process (a nonequilibrium effect), in addition to an increased wettability arising from long-range electrostatic polymer–surface interactions.

## 1. Introduction

The production of thin films and coatings is important for many commercial applications, e.g., coatings, dielectric layers, resist layers for lithography, electronic packaging, and lubricating surfaces.<sup>1,2</sup> Contemporary coatings technologies require increasingly thinner polymeric films. The ability to produce useful and uniform coatings depends on the wettability and adhesion of the polymer to the substrate. Control of film wetting properties is important since “dewetting” exposes the underlying substrate and compromises film barrier properties,<sup>3</sup> in addition to producing surface roughness and defects that may be deleterious to the performance of the polymer film.

Dewetting of polymeric films can be prevented by modifying the equilibrium polymer surface interactions or by “frustrating” the dewetting process through the formation of a glassy polymer film. Controlling the equilibrium spreading properties typically involves a surface treatment of the substrate or in some instances a modification of the polymer, or both. However, a modification of the polymer can cause nonequilibrium effects as well, such as shifting the glass transition ( $T_g$ ) in thin films, which can dramatically influence the dewetting kinetics. In these more complex situations, where kinetic and equilibrium effects are competing, it is difficult to attribute a definite cause to the observed effect of suppressed dewetting.

Polymers containing a modest amount of ionic functionality (e.g.  $<15$  mol %) are often referred to as ionomers,<sup>4</sup> and this terminology is adopted in the present paper. Here, we have chemically modified low molecular weight polystyrene to synthesize different ionomers by introducing bonded metal sulfonate groups along the polymer chain with the intention of controlling

the wettability of the polymer on an inorganic oxide surface such as silicon oxide. This modification is expected to affect the wetting characteristics of these films.

Most studies on preventing dewetting involve a surface treatment in the form of a chemical or physical modification of the substrate. There has been some success in surface treatments involving chemical modification, such as HF passivation,<sup>5</sup> or by using grafted homopolymer,<sup>6</sup> or random copolymers,<sup>7</sup> or simply by increasing surface roughness.<sup>8</sup> A more versatile method in recent years involves using functionalized self-assembled monolayers or SAMs,<sup>9</sup> since it allows the surface functionality to be varied almost continuously. In contrast to the above methods, there have been far fewer studies involving modification of the polymer to alter its wetting properties. An apparent drawback of such a process is that the film properties are somewhat altered, yet there may be numerous applications where improving the film adhesion properties is the main concern.

A thermodynamically unstable polymer film can be mechanically deposited onto a substrate (e.g. by spin coating<sup>10</sup>) to produce a uniform film that may be frozen (e.g. at room temperature) by virtue of being quenched below its glass transition temperature,  $T_g$ . Typically, annealing such a film above its  $T_g$  will cause the film to dewet from the substrate. The dewetting kinetics is controlled by a number of factors such as film thickness and temperature<sup>11,12</sup> and involves both equilibrium and nonequilibrium effects. At equilibrium, the dewetting tendency of a film is characterized by a spreading coefficient  $S$ .<sup>3,13</sup>

$$S = \Gamma_s - (\Gamma_{sp} + \Gamma_p) \quad (1)$$

where  $\Gamma_s$  and  $\Gamma_p$  are the surface free energies of the solid substrate and polymer respectively, and  $\Gamma_{sp}$  is the interfacial free energy between the polymer, and the substrate. When the films are not ultrathin or -thick, the film is considered wettable when  $S > 0$  and partially

\* To whom correspondence should be addressed.

<sup>†</sup> University of Connecticut.

<sup>‡</sup> National Institute of Standards and Technology.

<sup>®</sup> Abstract published in *Advance ACS Abstracts*, December 15, 1997.

wettable when  $S < 0$ .<sup>14</sup> It is believed that capillary forces are responsible for partial wettability, but long range forces are required for complete wetting; i.e.,  $S > 0$ .<sup>14,15</sup> For  $S < 0$ , the film will dewet by nucleation and growth of holes, and the film will eventually break up into a patterned arrangement of droplets with an equilibrium contact angle given by Young's equation:

$$\cos \theta = (\Gamma_s - \Gamma_{sp})/\Gamma_p \quad (2)$$

It has been predicted that a nonwetting ( $S < 0$ ) ultrathin film may break up by a spinodal decomposition mechanism<sup>14</sup> (i.e., thermal amplification of capillary waves), rather than by nucleation and growth. In contrast, nonwetting ultrathick films ( $\approx \text{mm's}$ ,  $S < 0$ ) may be metastable due to the effect of gravity and dewetting must be externally induced, e.g., by nucleating a hole in the film.<sup>16</sup> For  $S > 0$ , the film is usually stable, but below a critical thickness the film may dewet by a nucleation and growth process.<sup>14</sup>

Previous studies have investigated the equilibrium wetting properties of polymers on chemically modified substrates (e.g. by HF etch, grafting self-assembled monolayers).<sup>9,17–19</sup> Typically the contact angle is taken as a measure of the surface and interfacial energies of the system based on eq 2. Most studies<sup>19</sup> involve unentangled polymers to exploit faster dewetting kinetics and to avoid nonequilibrium effects. The kinetics of dewetting of spin-coated thin polystyrene films on a silicon oxide substrate has been studied extensively by Reiter and co-workers.<sup>20–23</sup> Note that a silicon surface is typically covered with a  $\sim 1\text{--}2$  nm thick layer of silicon oxide, so it is the latter that is the substrate of interest (notwithstanding the potential influence of long range forces). Sharma and Reiter<sup>23</sup> have identified three basic stages of dewetting in thin polymer films less than 60 nm thick: (1) rupture, (2) expansion and coalescence of dewetted hole areas to form polygons, and finally (3) breakup of polygons into droplets of the film. Additionally, fingering instabilities were seen on low wettability substrates.

There have been far fewer studies on suppression of dewetting in systems where nonequilibrium kinetic effects are present, especially those involving a chemical modification of the polymer. In the absence of a clear distinction between equilibrium and nonequilibrium kinetic effects, the term "suppression of dewetting" refers to either a slowing down of dewetting kinetics (nonequilibrium) or inhibition of dewetting through a change of polymer surface interaction (equilibrium).

A modification of the equilibrium polymer-surface interaction can be expected to arise from enhanced ion-dipole interactions between the metal cation of the ionomer and the silicon oxide which decreases  $\Gamma_{sp}$ , and consequently increases wettability of the polymer via eq 1. For a sufficiently large reduction of  $\Gamma_{sp}$ , a positive spreading coefficient ( $S > 0$ ) may in fact be achieved, and the film will be thermodynamically stable. Nonequilibrium modification effects come about through intermolecular association of the ionic groups which reduce the mobility of the ionomer molecules in the melt.<sup>24</sup> This effect should retard dewetting kinetics of the polymer in a manner similar to increasing molecular weight or the entanglement density of the polymer. A high degree of association may produce a behavior analogous to a cross-linked polymer where the entanglements are permanently fixed and dewetting cannot

occur. Thus, suppression of dewetting may arise from kinetic effects<sup>25–27</sup> without the formation of any specific polymer-substrate complex.

Self-aggregation of an ionomer may also restrict the ability of the polar ionic species from interacting with a polar substrate even where such an interaction appears to be favorable. In this regard, we note that an as-spun-cast film of an ionomer is expected to have negligible inter- and intramolecular association when the films are prepared from solutions containing a significant percentage of a polar cosolvent, such as an alcohol, which inhibits association of the metal-sulfonate groups in solution.<sup>28</sup> Intermolecular association of the ionic groups is expected to occur upon annealing the film, so that dewetting may be kinetically retarded after an initial dewetting period during which the intermolecular associations form. This may produce "frustrated dewetting."

In previous papers,<sup>29,30</sup> we have characterized specific intermolecular complexation between the metal cations and the carbonyl ( $\text{O}=\text{C}<$ ) group in sulfonate ionomer/polyamide blends. Since both C and Si are group IVA elements and Si has less electron withdrawing power, a similar, if not stronger, intermolecular complexation is expected between metal ions and the  $\text{O}=\text{Si}<$  group. Our goal in this study is to examine the effect of association between the polymer molecules in slowing-down the dewetting kinetics (a nonequilibrium effect), and the role of coordination between the metal cation and the oxide substrate in reducing the interfacial free energy,  $\Gamma_{sp}$ , leading to increased wettability (an equilibrium effect). We first perform a detailed study of the equilibrium dewetting characteristics of the parent unmodified low molecular weight polystyrene to provide a base line for comparison with the anticipated nonequilibrium effect for the sulfonated PS films. Using X-ray reflectivity and atomic force microscopy (AFM), we study the dewetting kinetics and measure the equilibrium contact angle of dewetting profiles, respectively. We then investigate the sulfonated PS where the lithium sulfonate concentration in the polymer is varied and replace the lithium cation with zinc to gain insight on the cation dependence of polymer-substrate interaction.<sup>29,30</sup> Finally, we correlate these wetting properties with rheological properties of the modified and unmodified polymer. Through these measurements, we demonstrate that it is possible to finely tune the effective wettability of thin polymer films on inorganic oxide substrates by introducing a metal-ion complex into the polymer.

## 2. Experimental Section

**A. Materials.** The acid form of lightly sulfonated polystyrene (H-SPS) samples were prepared by sulfonating a narrow molecular weight distribution polystyrene (Pressure Chemical Co.,<sup>31</sup>  $\text{MW} = 4000$ ,  $M_w/M_n = 1.06$ ) with acetyl sulfate in 1, 2-dichloroethane at 50 °C.<sup>32</sup> That reaction produces random substitution along the chain primarily at the para-position on the phenyl ring. The sulfonation level was determined by titration of H-SPS in a mixture of 90% toluene/10% methanol (v/v) and is reported here as mol %, which is defined as the average number of sulfonate groups in 100 styrene repeat units. Lithium and zinc salts of the lightly sulfonated polystyrene, Li-SPS and Zn-SPS, respectively, were prepared by neutralizing the H-SPS in a 90% toluene/10% methanol solution with 20% excess of a methanol solution of the appropriate metal acetate. The neutralized polymers were then isolated from solution by steam stripping, filtered, washed, and dried under vacuum. Li-SPS and Zn-SPS with

sulfonation levels of 0.8, 1.5, 2.3, 7.0, and 10 mol % were prepared.

A free-radical polymerized polystyrene with  $M_n = 5000$  was used to prepare sulfonated polystyrene ionomers for dynamic mechanical analysis. Sulfonation was carried out to a level of 2.65 mol % as described above, and the sodium, zinc, and manganese salts were prepared by neutralizing the sulfonic acid derivative with the appropriate metal acetate.

**B. Specimens.** Specimens for the optical microscopy and X-ray reflectivity measurements were prepared by spin-coating 1% by mass of PS in toluene or 1% by mass of Li-SPS or Zn-SPS in a mixture of 90% toluene/10% methanol onto an optically flat and polished silicon wafer (Semiconductor Processing, Inc.<sup>31</sup>) at 2000 rpm. This produced a uniform polymer film between 30 and 40 nm thick. Prior to spin coating the polished silicon wafers were prepared as follows. Each wafer was cleaned in a bath of a mixture of 70% sulfuric acid and 30% hydrogen peroxide by volume at an elevated temperature of 80 °C for a minimum of 60 min. Subsequently, the wafers were thoroughly rinsed in deionized water, blown dry with nitrogen, and then placed in a vacuum oven for approximately 30 min at room temperature. This procedure is known to remove the initial hydrocarbon contamination layer and to oxidize or partially hydroxylate the silicon surface, whose stoichiometric nature was not characterized. The spin-coated samples were annealed at several different temperatures in a preheated vacuum oven for designated periods of time and then quenched to room temperature.

**C. Measurements.** X-ray reflectivity (XR) measurements were performed on a fixed anode Scintag XDS 2000 reflectometer<sup>31</sup> and all measurements were carried out at room temperature. XR can be used to characterize the surface roughness of thin films on a flat surface with subnanometer resolution and with an estimated error of 0.1–0.2 nm. The reflectivity spectrum from a smooth and uniform film on a flat surface exhibits Kiessig interference fringes,<sup>33,34</sup> an oscillation of the reflected intensity as a function of the  $z$ -component wavevector of the incident X-ray. Since dewetting of the film causes an increase in the roughness of the film–air interface, the interference fringes in the reflectivity spectrum become progressively smeared out as dewetting proceeds. Therefore, the parameter describing the film–air interfacial roughness,  $\sigma_a$ , is a measure of the extent of dewetting at early stages. A small value of  $\sigma_a$  (typically <0.5 nm) represents a smooth and uniform film while a relatively large value of  $\sigma_a$  represents a completely dewetted film that no longer has interference fringes in its reflectivity spectrum.

A single layer model whose air–polymer interfacial roughness is described by an error function was used to fit the XR data from the polystyrene and sulfonated polystyrene ionomers films. The error function was chosen to represent a Gaussian broadening process at the interface, but it by no means represents a unique functional fit to the data. The ambiguity in uniqueness, however, does not affect our interpretation of the data. More detailed fits were considered by Reiter et al.<sup>21</sup> All data involve adjusting the air–film interfacial roughness,  $\sigma_a$ , and to a much lesser extent, the interfacial roughness between the substrate and the polymer,  $\sigma_s$ .

XR characterizes the surface roughness of dewetting films through variation of the average polymer density normal to the film surface. As a supplement to XR, optical microscopy (OM) was used to observe the dewetting phenomena on the surface. Optical micrographs were taken with a Nikon Optiphot reflection microscope<sup>31</sup> equipped with an automatic exposure setting camera.

AFM measurements were also performed to characterize the surface topology of the dewetting films. Measurements were performed in contact mode with a Topometrix instrument<sup>31</sup> using a silicon tip in air with applied forces in the range of  $\approx 10$ –40 nN. Scanning was performed at different speeds (0.1–2 Hz) and scan sizes (50–100 nm) to check for reproducibility and generality of results.<sup>35–37</sup> Results are presented as obtained without filtering. The zero height in all of the AFM line profiles is artificially set by the program software and does not refer to the substrate surface.

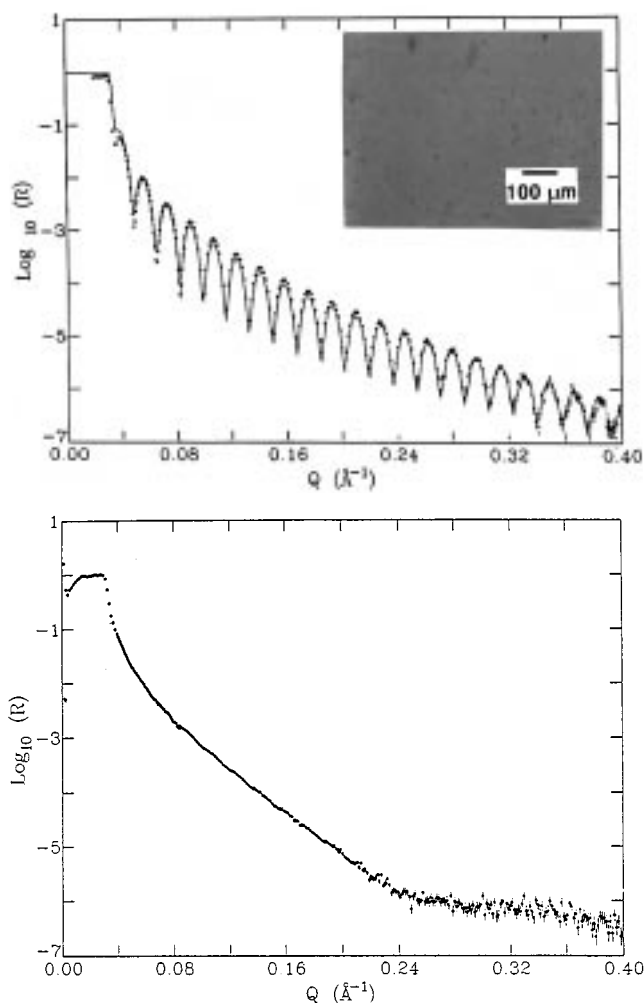


**Figure 1.** (a) X-ray reflectivity (XR) from an as-cast  $\sim 30$  nm thick PS film spun-cast on a silicon. The undamped oscillations are indicative of a smooth film, as confirmed by the optical micrograph (OM) image shown in the inset. The black spots in the OM are dust particles. (b) XR after annealing for 20 h at 115 °C. The oscillations are now completely damped out as a result of dewetting of the film (see Figure 2.)

Dynamic mechanical properties of the 2.65 mol % ionomers were measured with a Rheometrics System 4 mechanical spectrometer<sup>31</sup> using 25.4 mm parallel plates and the oscillatory shear mode. Strain sweeps were made to identify the limits of linear viscoelastic response, and all measurements were made in the linear region. Measurements were made at a constant frequency of 1 Hz over a temperature range of 90–190 °C.

### 3. Results

Results are categorized in four sections. Section A presents measurements characterizing dewetting of unmodified polystyrene samples. These provide a reference base with which to compare with the dewetting of the ionomers. Section B describes the suppression of dewetting observed with Li-SPS, and section C discusses results obtained for Zn-SPS. Finally, section D compares the dewetting results of sections A, B, and C to the bulk viscoelastic behavior of SPS ionomers.

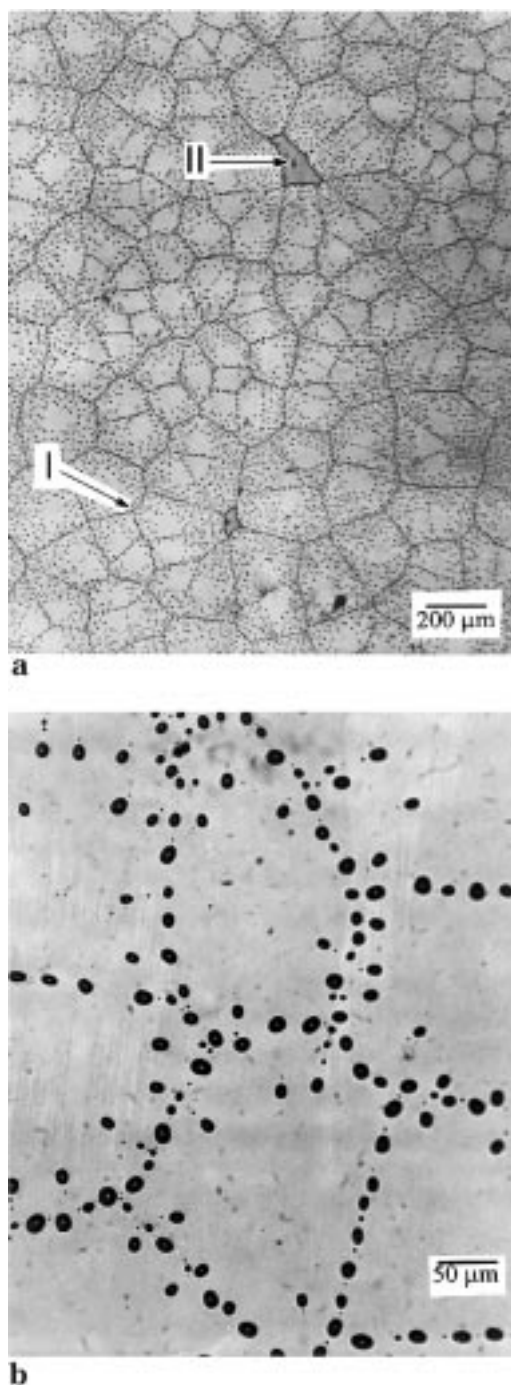
**A. Unmodified PS films ( $M_w \approx 4000$ ).** Figure 1a shows XR of an as-cast  $\approx 30$  nm thick PS film. The relatively undamped interference fringes are indicative of a uniform and smooth film on the silicon substrate. A single layer model fit yielded an air–film roughness,  $\sigma_a \approx 0.55$  nm and a film–substrate roughness,  $\sigma_s \approx 0.35$

nm. The OM inset of Figure 1a illustrates a uniform surface, consistent with the XR data. All of the as-cast films, whether modified or not, exhibited similar uniformity as measured by XR and OM.

The PS film showed characteristics of classic dewetting ( $S < 0$ ) for low wettability surfaces. Figure 1b shows XR from the PS film after annealing for 20 h at 115 °C. The spectrum of interference fringes is completely damped, indicative of a very rough surface, such as one caused by complete dewetting of the film. A very large value of  $\sigma_a$  would be required to describe the air–film surface roughness for this case. Parts a and b of Figure 2 are OM of the above annealed PS film at low and high magnification, respectively. The low magnification micrograph, Figure 2a, shows a constellation of satellite droplets in the vicinity of a cellular array of dewetted droplets. Such a dewetting pattern has been reported by Reiter et al. to occur on low wettability surfaces<sup>19</sup> and reflects a competition between breakup of film along the rim through a rim instability and rim expansion kinetics. The “cellular” structure, which is hexagonal on average, resembles a 2-D Voronoi tessellation pattern composed of dewet PS droplets.<sup>22</sup> It occurs at an advanced stage of dewetting. The two optical micrographs of parts a and b of Figure 2 illustrate that annealing at 115 °C for 20 h is sufficient to dewet a relatively low molecular weight PS thin film from a silica surface.

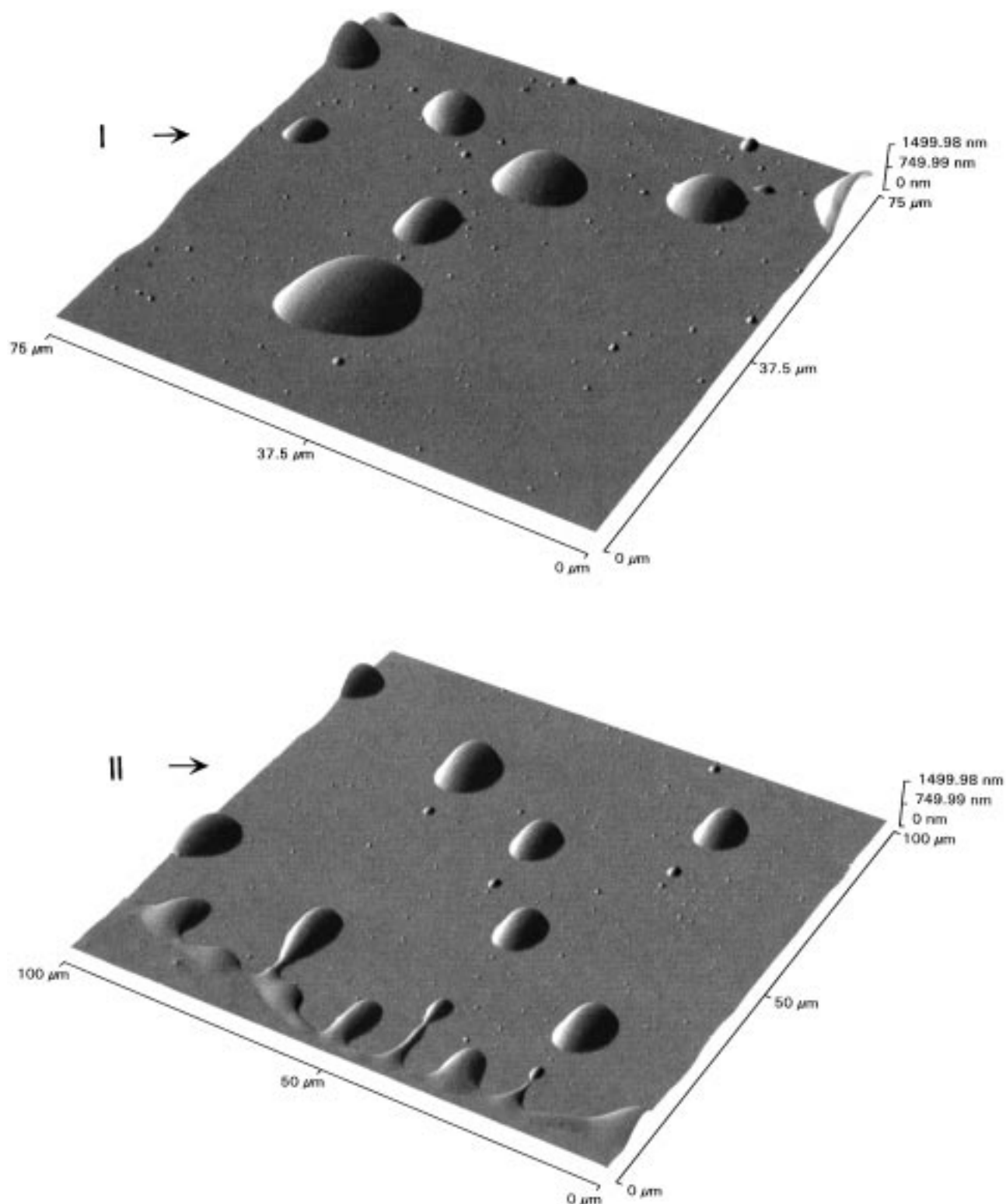
Most of the PS film forms tiny droplets that assume an array pattern, with junction points as illustrated by the arrow marked **I** in Figure 2a, and seen more clearly in Figure 2b. Dewetting exposes large areas of the silicon surface to the air. There are, however, some patches of the original film left that did not dewet, as illustrated by arrow **II** in Figure 2a. Figure 3 shows 3D AFM images of the regions marked **I** (Y-shaped junction of an array pattern) and **II** (edge of film breaking-off into droplets) in Figure 2a. Figure 4 provides a top view of the Y-shaped junction (**I**) of Figure 3, with lines profiles marked a, b, and c, drawn across different dewet droplets of the Y-shaped junction. Line a is drawn on a droplet of diameter  $\approx 12$  nm, and it has an equilibrium contact angle,  $\theta_e \approx 15.5^\circ$ . Neighboring droplets (lines b and c) of diameter  $\approx 7$  and 18 nm respectively show only a nominal  $\pm 0.1^\circ$  variation in  $\theta_e$ . Thus, the droplet contact angle is not related to the droplet size, as suggested by eq 2 for droplets at equilibrium. We estimate  $\Gamma_{sp}$  to be less than 5 dyn/cm based on known surface tensions of silicon oxide and low molecular weight polystyrene.<sup>9</sup>

Figure 5 is a top view of the AFM micrograph of the region marked **II** in Figure 3, enclosing a small section of the original film with mostly dewet area. The AFM picture of Figure 5 indicates a clear rim between the dewet droplet and the continuous film. The rim is seen breaking off into droplets by fingering instabilities.<sup>23</sup> Sharma and Reiter<sup>23</sup> suggest that these long fingers develop from the retracting rim for dewetting on low wettability surfaces. It is hypothesized that these fingers do not retract as fast as the moving rim and break up of the resulting fluid threads by a Rayleigh type instability, thus giving rise to a constellation of satellite droplets. Line profile a is drawn across an isolated droplet, b across a “budding” droplet, and c at the rim between two fingering instability. The isolated droplet has a contact angle that is similar to the junction droplets of Figure 4. Line profile b in Figure 5 across



**Figure 2.** OM from the annealed (20 h at 115 °C) regular PS film. a) Low magnification image depicting mostly dewet droplets (e.g. see area **I**), and few areas of the remnant film (e.g. see area **II**); (b) higher magnification of a dewet droplet area showing the polygonal pattern and junction points.

the budding droplet has a contact angle with silicon oxide of  $\approx 9.8^\circ$ , while the rim between two “fingering droplets” has a contact angle of only  $\approx 3.5^\circ$ . Thus, it appears that the droplets attain their equilibrium contact angle only after breaking off from the film. The height difference on either sides of the rim from line profile c in Figure 5 roughly corresponds to the film thickness of  $\approx 30$  nm, in agreement with X-ray reflectivity measurements of initial film thickness. The average distance between fingering instabilities across the rim is  $\approx 10$  nm, so that the wavelength of the rim instability discussed above and the resulting droplets have dimensions of the same order. The satellite

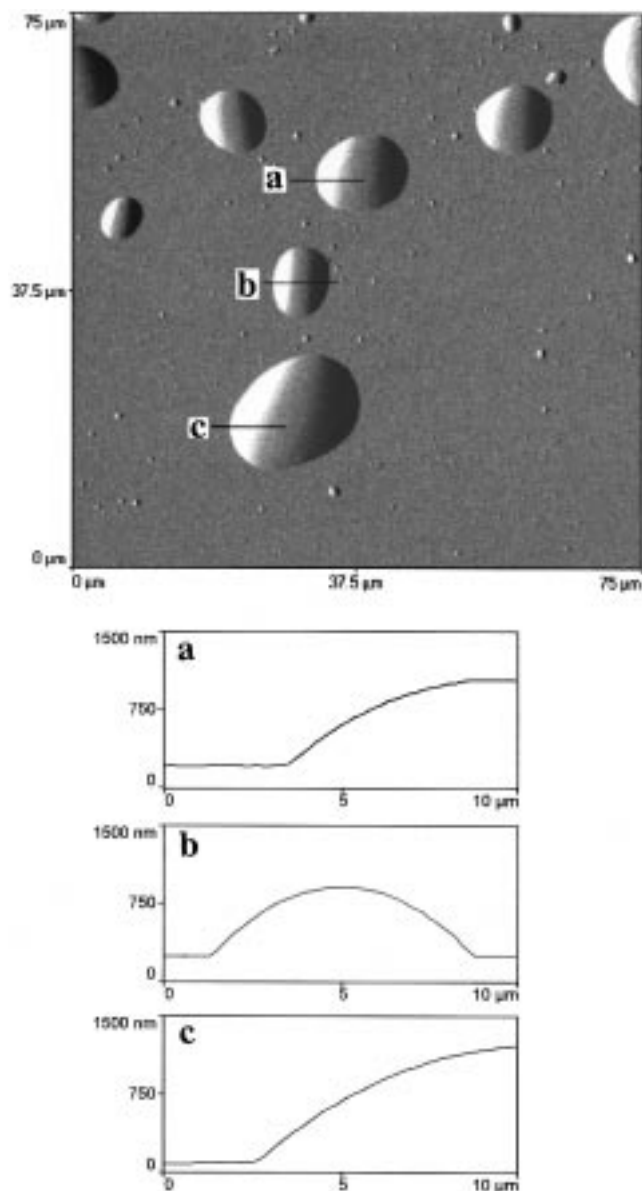


**Figure 3.** Atomic force microscopy (AFM) image of slant view of regions marked **I** and **II** in Figure 2, depicting the Y-junction point of a polygon formed by dewet droplets and the boundary between remnant film and dewet area, respectively.

droplets produced by the rim instability are fairly monodisperse in size, unlike those formed at junction points as in Figure 4. In conclusion, very thin low molecular weight polystyrene films dewet the silica surface once the PS chains obtain sufficient mobility at elevated temperatures.<sup>20–22</sup>

**B. Li-SPS Films.** XR from an as-cast 2.3 mol % Li-SPS film was very similar to that from the unmodified PS film (Figure 1a). The single layer model fitting

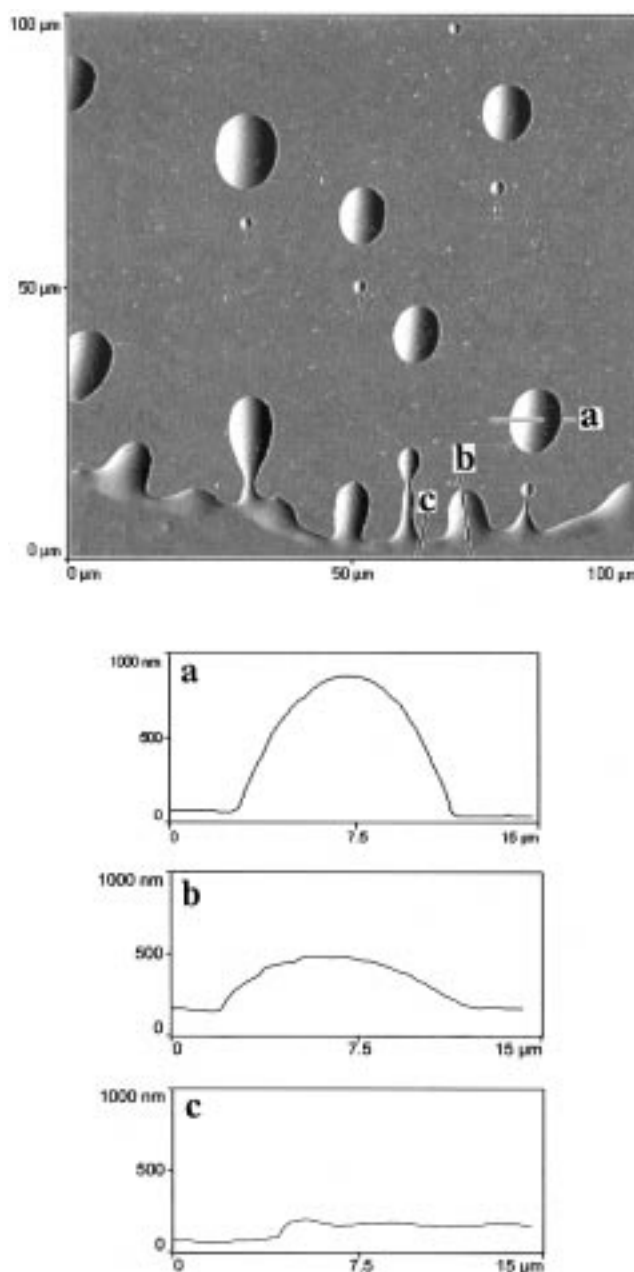
yielded  $\sigma_a \approx 0.8$  nm and  $\sigma_s \approx 0.4$  nm, indicating a uniform and smooth film and is typical of all the sulfonated polystyrene ionomer films in their as-cast state. Figure 6 shows the reflectivity spectrum from the 2.3 mol % Li-SPS film after it was annealed under identical conditions as the PS film, i.e., at 115 °C for 20 h. Unlike the PS, where the interference fringes were totally smeared out upon annealing, only a partial damping of the oscillations occurred for the low sul-



**Figure 4.** AFM of top view of Y-junction region **I** of Figure 2 with line profiles across dewet droplets of different sizes ( $b < a < c$ ). The zero height in all of the AFM line profiles is artificially set by the program software and does not refer to the substrate surface.

fonation level ionomer, which indicates a more moderate roughening, as occurs at early stages of dewetting. The single layer model fit yielded a  $\sigma_a$  of only 1.7 nm. This is in sharp contrast to the advanced stage of dewetting observed for PS of the same molecular weight and thermal history. The inset of Figure 6 shows an optical micrograph of the annealed 2.3 mol % Li-SPS film. Clearly, there are no "cellular" structures, in contrast to the dewetting pattern of the pure PS film shown in Figure 2. The OM inset in Figure 6 shows small holes on the Li-SPS film surface, similar to those observed by Reiter and Sharma at very early stages of film dewetting.<sup>23</sup> Thus, it appears that the kinetics of dewetting are inhibited in the 2.3 mol % Li-SPS film compared to a PS film of similar thickness.

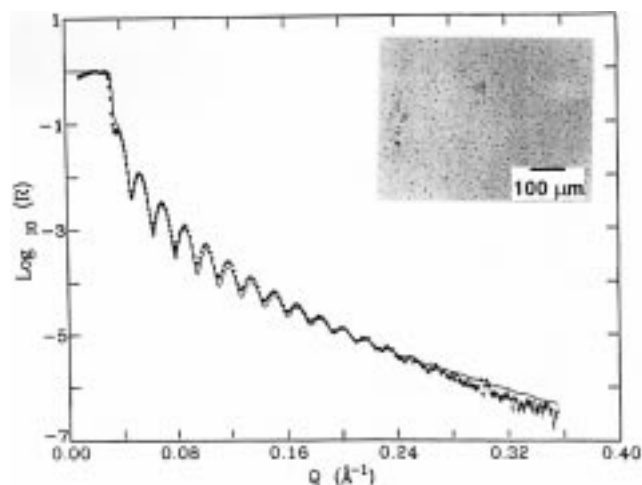
Figure 7 shows the top view of an AFM micrograph of the 2.3 mol % Li-SPS annealed at 115 °C for 20 h. It illustrates the formation of a hole in the film of diameter  $\approx 35$  nm and surrounded by a rim. The line profile of



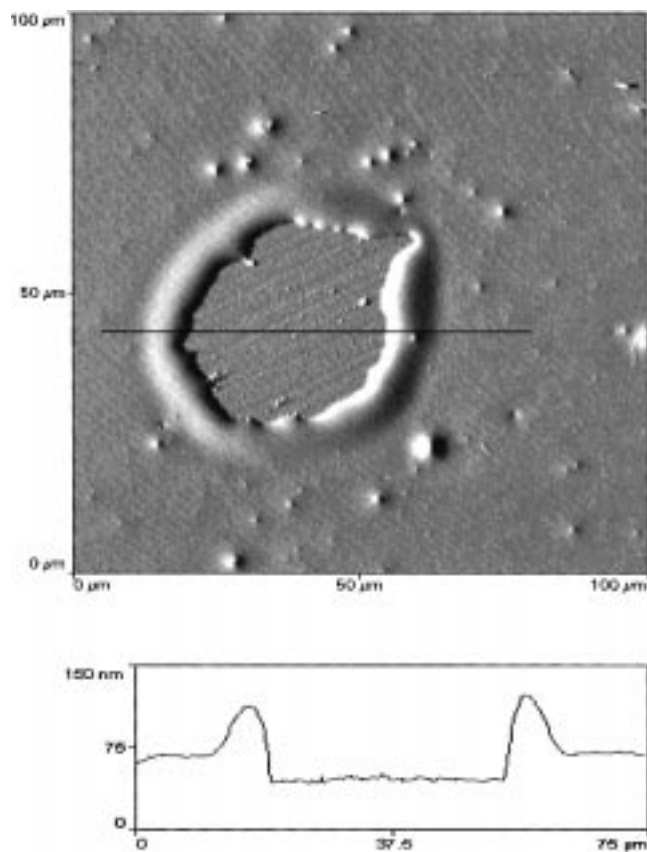
**Figure 5.** AFM of top view of boundary area **II** of the remnant film in Figure 2 with line profiles marked: (a) separated droplet; (b) a budding droplet caused by fingering instabilities; (c) neck between two budding droplets.

Figure 7 indicates the elevated rim around the crater with a relatively small dynamic contact angle of  $\approx 2.4^\circ$ . As before, the height difference between the crater and the outer parts of the film corresponds to the film thickness of  $\approx 25$  nm. Evidently, the introduction of 2.3 mol % of Li-sulfonate groups into PS dramatically slows down the dewetting process since such hole formation is typically observed during early stages of dewetting. As discussed in the introduction, this effect could be an equilibrium effect through enhanced coordination between the metal cation and the silicon oxide surface or a nonequilibrium effect associated with inter and intra molecular association and complexation.

We observed that when the film was annealed at a higher temperature of 140 °C for 72 h, the X-ray reflectivity oscillations were completely damped, similar to Figure 1a for PS. Thus, the dewetting could be



**Figure 6.** XR from an annealed (20 h at 115 °C) 2.3 mol % Li-SPS film. The damping of oscillations is indicative of a limited dewetting of the film. The dewet areas can be seen in the OM inset as dark spots.



**Figure 7.** AFM top view of a dewetting hole in a 2.3 mol % Li-SPS film annealed for 20 h at 115 °C. The line profile drawn across the hole clearly shows the rim around the expanding hole. The film thickness can also be estimated to be on the order of 30 nm.

carried out to completion for the 2.3 mol % Li-SPS. The droplets were of various shapes and sizes, which may be a consequence of the variability of the number of sulfonate groups per chain or of a random spacing of the ionomer-substrate complexes in the plane the silicon oxide surface. The sulfonation reaction produces random sulfonation of the styrene groups, which results in variability of sulfonate groups per chain. Because of the low degree of polymerization ( $dp \sim 39$ ) of the polystyrene used, some chains will have no sulfonate

groups, while others will have more than the average sulfonation level. The concentration of unsulfonated chains is expected to be most acute for the lowest sulfonation level (2.3 mol %), which on average has one sulfonate per chain. The distribution of sulfonate groups and/or the position of the complexes may also account for the large areas of film remnants after dewetting. Not surprisingly, the contact angle of the dewet droplets exhibited a lot of variability about an average of  $\sim 15^\circ$ . Assuming a quasi-equilibrated situation, the SPS-silicon oxide interfacial tension is only marginally reduced for the 2.3 mol % sulfonation level samples.

Annealing had different effects on films with different sulfonation levels (and different cations, as is described in section C). The results of fitting XR from thin films of Li-SPS with different sulfonation levels are listed in Table 1. From an equilibrium standpoint, and for fixed metal cation, increasing the sulfonation level should increase the total number of polymer-substrate intermolecular complexes, thereby decreasing  $\Gamma_{sp}$  and leading to more stable films. While it is not possible to establish a definite trend for sulfonation levels below 2.3% within the error bars in Table 1, a suppression of dewetting or roughening in the 7.0 and 10.0 mol % sulfonation level films is evident. However, this does not imply that a rearrangement of molecules or surface segregation of ionomer end-groups does not occur upon annealing. More detailed analysis of the XR data might reveal such changes, however such an analysis is out of the scope of the present paper. An optical micrograph of a 7.0 mol % Li-SPS film was featureless, similar to the inset of Figure 1a, after the film was annealed at the higher temperature of 140 °C for 3 days. No evidence of dewetting was found by OM or XR in films with higher sulfonation levels as well.

**C. Zn-SPS Films.** The effect of the metal cation ionization potential on dewetting was investigated by changing from a  $Li^+$  to a  $Zn^{2+}$  cation with similar sulfonation levels. In all cases, annealing had a much smaller roughening effect on films containing zinc cations than lithium cation containing films, as observable from Table 1. Zinc has a much stronger electron withdrawing power compared to lithium, and hence, complexation with an electron donor such as a silicon oxide surface should be much stronger. Thus, the equilibrium wettability or enhancement of interfacial adhesion should be even more effective for zinc sulfonate. Figure 8 gives the reflectivity from the 2.3 mol % Zn-SPS film after being annealed identically to the PS and 2.3% Li-SPS films, i.e. for 20 h at 115 °C. The single layer model fitting yielded  $\sigma_a \approx 0.75$  nm, and almost no time dependence to dewetting was detected by X-ray reflectivity.

It should be pointed out that a decrease in either  $\Gamma_p$  or  $\Gamma_{sp}$  of eq 1 promotes wettability. Introduction of a small amount of metal sulfonate groups may lower  $\Gamma_p$ , the surface energy of polystyrene, but it does not undermine the effects of intermolecular complexation. If the wettability improvement were solely due to a surface energy decrease of the polystyrene as a result of sulfonation, it should have had a comparable effect on Li-SPS and Zn-SPS films. The fact that Zn-SPS films have significantly better wettability indicates that polymer-substrate intermolecular complexation (reduction of  $\Gamma_{sp}$ ) probably plays a crucial role for enhancing wettability in such systems.



**Table 1.** Values of  $\sigma_a$  and  $\sigma_s$  Calculated from X-ray Reflectivity Measurements for Annealed SPS Films Spin-Cast onto Silicon Wafers

annealing condition		as-cast		115 °C for 20 h		140 °C for 3 days	
% sulfonation	salt	$\sigma_a$ (nm)	$\sigma_s$ (nm)	$\sigma_a$ (nm)	$\sigma_s$ (nm)	$\sigma_a$ (nm)	$\sigma_s$ (nm)
0.8	Li <sup>+</sup>	0.87	0.30	1.30	0.41	N/A <sup>b</sup>	N/A
1.5	Li <sup>+</sup>	0.50	0.32	1.60	0.42	N/A	N/A
2.3	Li <sup>+</sup>	0.80	0.40	1.70	0.40	N/A	N/A
7.0	Li <sup>+</sup>	0.80	0.40	0.88	0.46	N/A	N/A
10.0	Li <sup>+</sup>	<i>a</i>	<i>a</i>	<i>a</i>	<i>a</i>	0.80	0.47
0.8	Zn <sup>2+</sup>	0.75	0.31	0.80	0.31	N/A	N/A
1.5	Zn <sup>2+</sup>	0.75	0.33	1.10	0.35	N/A	N/A
2.3	Zn <sup>2+</sup>	0.60	0.33	0.75	0.33	N/A	N/A
7.0	Zn <sup>2+</sup>	0.75	0.38	0.78	0.48	0.78	0.46
10.0	Zn <sup>2+</sup>	0.85	0.55	0.85	0.60	0.85	0.55

<sup>a</sup> Reflectivity data could not be fit by a single layer model. <sup>b</sup> N/A: Experiment not run.

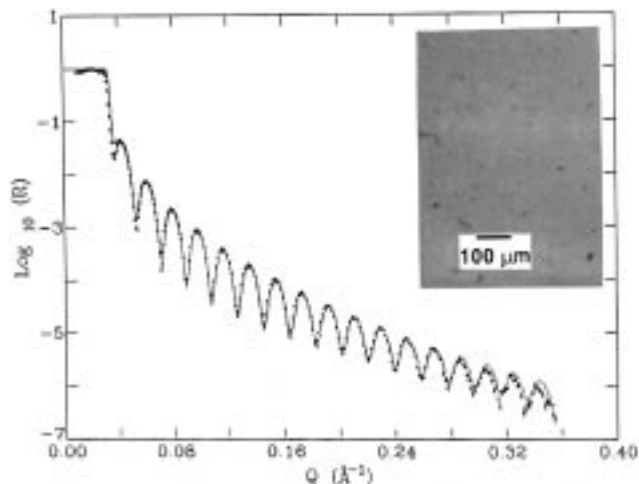


**Figure 8.** XR from a 2.3 mol % Zn-SPS film after being annealed for 20 h at 115 °C. The XR did not change when the film was annealed for 72 h at 140 °C, illustrating an enhanced film stability compared to the PS and 2.3 mol % Li-SPS. The corresponding homogeneous optical micrograph of the 2.3 mol % Zn-SPS is shown in the inset.

For the 2.3 mol % Zn-SPS film, the OM inset of Figure 8 shows that dewetting does not occur even after annealing for 3 days at 140 °C, similar to the 7.0 and higher mol % Li-SPS samples. This is contrasted with the 2.3 mol % Li-SPS material which completely dewet under similar annealing conditions. Thus, complete suppression of dewetting with the more electronegative Zn cation forming complex is evident. From previous studies<sup>29,30</sup> we know that the strength of this type of coordination varies with the metal ion type, thus providing a mechanism for finely controlling the dewetting behavior of polymer films by using different metal cations.

**D. Bulk Rheology Data.** As discussed in the Introduction, there are two possible explanations for a suppression of the dewetting kinetics with sulfonation. Although it is tempting to attribute the improved wetting to long-range dipolar interactions (complexation) with the silicon oxide surface, one cannot dismiss the possibility of the frustration of dewetting arising from association of ion-dipoles in the ionomer. This effect increases the effective molecular weight of the polymer and the effective "entanglement" density. Even though the molecular weight of our starting polystyrene ( $M_n = 4000$ ) was far below the critical molecular weight for entanglement coupling for polystyrene ( $M_c \sim 35\,000$ ), ionic interactions significantly perturb the viscoelastic behavior of the polymer and may act similar to entanglements in the sense of leading to a similar complex

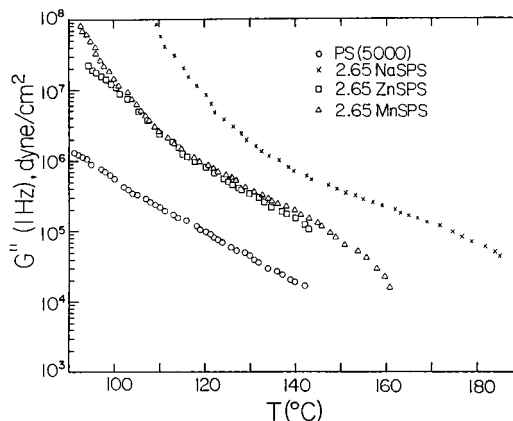


**Figure 9.** Dynamic loss modulus at a frequency of 1 Hz vs temperature for PS ( $M_w = 5000$  g/mol) and its 2.65 mol % sulfonate ionomers.

viscoelasticity as entangled polymers. For example, Figure 9 compares the dynamic loss modulus vs. temperature behavior of several salts of a sulfonated polystyrene ionomer (2.65 mol % sulfonation) with the parent polystyrene ( $M_w \sim 5000$ ). Note that for this low molecular weight polymer, even a modest sulfonation level increases the viscosity ( $\eta' = \omega G''$ , where  $\eta'$  is the dynamic viscosity and  $\omega$  is the experimental frequency) by about 1–2 orders of magnitude for  $T > T_g$ . That effect is due to association of the ionic species (an apparent entanglement or dynamic cross-link depending on which terminology one prefers) and it is dependent on the choice of the cation.

The Na<sup>+</sup> salt data shown in Figure 9 gives rise to a greater increase of the viscosity and the dynamic modulus (data not shown here) than either the Zn<sup>2+</sup> or Mn<sup>2+</sup> salts. The latter two transition metal ions have higher ionic potential ( $q/r$ , where  $q$  = the ionic charge and  $r$  = the ionic radius) than Na<sup>+</sup>, which is apparently the important factor in substrate-intermolecular complexation enhanced wetting. The wetting results described above, for which the Zn<sup>2+</sup> salt of SPS showed better resistance to dewetting than the Li<sup>+</sup> salt, are consistent with the relative values of the ionic potential of the two cations,  $q/r = 27.8$  and 14.1, respectively, suggesting modifications of polymer surface interactions as the primary cause for enhanced wettability.

#### 4. Discussion

Several points of observation merit more a detailed discussion. The most important observation is that a light sulfonation of the polystyrene molecule dramatically improves the polymer's resistance to dewetting



from a silicon oxide substrate. The advantage of such a technique lies in its general applicability to a wide range of polymers and inorganic substrates. For example, metal sulfonate groups can be introduced into a variety of polymers, which can be accomplished either by direct sulfonation of a preformed polymer or by copolymerization of a low level of functionalized monomer with an unsaturated monomer. Direct sulfonation can be performed on a number of polymers including polystyrene,<sup>38,39</sup> EPDM,<sup>38,39</sup> polysulfone,<sup>40</sup> polypentenamer,<sup>39</sup> and perfluorinated polymers.<sup>41</sup> The copolymerization of sodium styrene sulfonate with isoprene, butadiene and styrene monomer, has also been reported,<sup>42–44</sup> respectively. For polyolefins, such as polyethylene, where metal sulfonate groups are difficult to introduce, one could substitute metal carboxylate groups for metal sulfonate groups. Metal carboxyl containing polymers can be obtained by copolymerization of acrylic or methacrylic acid with a vinyl or diene monomer followed by neutralization with metal hydroxides, acetates or similar salts.<sup>32</sup>

The sulfonation approach to enhancing wettability is of wide application because silica is a commonly encountered substrate. Various metals can be used in the metal-containing groups. Since the strength of the intermolecular complexation varies with the metal, the interfacial adhesion can be "tuned" by varying the metal ion and sulfonation level.

The resistance to dewetting was strongly dependent on the sulfonation level and the cation used in neutralizing the ionomer. Two questions arise from this work: (1) Was the improved wetting a consequence of ion-substrate interactions or a manifestation of the effects of ionic aggregation on the viscoelastic properties of the polymer (i.e., increased relaxation times)? (2) If the improved wetting was due to ion-substrate interactions, can some general rules be formulated for choosing the cation to optimize the wetting/dewetting characteristics of the film? These two questions will be the study of future research.

The dewetting phenomena described in the previous section and the viscoelastic data shown in Figure 9 are too limited to be conclusive as to the origin of the dewetting suppression found in our measurements. Measurements of the dynamic modulus should allow us to calculate an effective "excess" entanglement density from the difference in modulus above  $T_g$  for the sulfonated polymers and the parent polystyrene. That modulus may be related to the molecular weight between cross-links, or in this case, between entanglements (i.e., ionic associations) analogous to classical rubber elasticity calculations.<sup>45</sup> We have previously characterized the effect of ionic association on the effective entanglement density or cross-linking of higher molecular weight sulfonated polystyrene ionomers in the bulk.<sup>46</sup> Since we are primarily concerned with how different ions affect the entanglement density, i.e., the apparent molecular weight of the ionomer, dewetting experiments will also be run on polystyrene homopolymer films with molecular weights comparable to the calculated apparent molecular weights of the ionomers to evaluate whether entanglements are responsible for the suppression of dewetting observed with the ionomers or whether the effect has its origin in the modification of the polymer surface interaction.

In summary, a suppression of dewetting of low molecular weight sulfonated polystyrene ionomers (SPS)

on inorganic silicon oxide substrates was observed using X-ray reflectivity, optical and atomic force microscopy. SPS thin films with controlled amounts of  $\text{Li}^+$  and  $\text{Zn}^{2+}$  metal counterions were compared to unmodified PS, which readily dewet the substrate. In  $\text{Li}^+$  films with low sulfonation ( $\approx 2.3$  mol %), dewetting was strongly suppressed, and no apparent dewetting was found for high sulfonation levels ( $\geq 7$  mol %). No dewetting was observed in ZnSPS films, even for low sulfonation levels. Bulk rheological data suggest that inter and intra molecular ionomer complexation may be additional important factors in retarding dewetting.

**Acknowledgment.** This research was supported by Polymer Program of the National Science Foundation (Grant DMR 9400862).

## References and Notes

- (1) Licari, J. J. *Plastic Coatings for Electronics*; McGraw-Hill Book Company: New York, 1970.
- (2) Cowie, J. M. G. *Polymer: Chemistry and Physics of Modern Materials*; Chapman and Hall: New York, 1991.
- (3) Wu, S. *Polymer Interface and Adhesion*; Marcel Dekker, Inc.: New York, 1982.
- (4) Fitzgerald, J. J.; Weiss, R. A. *Rev. Macromol. Chem. Phys.* **1998**, C28 (1), 99.
- (5) Sung, L.; Karim, A.; Douglas, J. F.; Han, C. C. *Phys. Rev. Lett.* **1996**, 76, 4368.
- (6) Henn, G.; Bucknall, D. G.; Stamm, M.; Vanhoorne, P.; Jerome, R. *Macromolecules* **1995**, 29, 4305.
- (7) Mansky, P.; Russell, T. P.; Hawker, C. J.; Mays, J.; Cook, D. C.; Satija, S. K. *Phys. Rev. Lett.* **1997**, 79, 237.
- (8) Tolan, M.; Vacca, G.; Wang, J.; Sinha, S. K.; Li, Z.; Rafailovich, M. H.; Sokolov, J.; Gibaud, A.; Lorenz, H.; Kotthaus, J. P. *Phys. B* **1996**, 221, 53.
- (9) Ulman, A. *An Introduction to Ultrathin Organic Films*; Academic Press: New York, 1991.
- (10) Weill, A.; Dechenaux, E. *Polym. Eng. Sci.* **1988**, 28, 945.
- (11) Srolowitz, D. J.; Safran, S. A. *J. Appl. Phys.* **1986**, 60, 247.
- (12) Sekimoto, K.; Oguma, R.; Kawasaki, K. *Ann. Phys. (N.Y.)* **1987**, 176, 359.
- (13) Jabbari, E.; Peppas, N. A. *Rev. Macromol. Chem. Phys.* **1994**, C34 (2), 205.
- (14) Brochard, F. W.; Daillant, J. *Can. J. Phys.* **1990**, 68, 1084.
- (15) Srolowitz, D. J.; Safran, S. A. *J. Appl. Phys.* **1986**, 60, 247.
- (16) Redon, C.; Brochard, F.; Rondelez, F. *Phys. Rev. Lett.* **1991**, 66, 715.
- (17) Nuzzo, R. G.; Fusco, F. A.; Allara, D. L. *J. Am. Chem. Soc.* **1987**, 109, 2358.
- (18) Whitesides, G. M.; Laibinis, P. E. *Langmuir* **1990**, 6, 87.
- (19) Reiter, G. *Langmuir* **1993**, 9, 1344.
- (20) Reiter, G. *Phys. Rev. Lett.* **1992**, 68, 75.
- (21) Reiter, G. *Macromolecules* **1994**, 27, 3046.
- (22) Stange, T. G.; Mathew, R.; Evans, D. F.; Hendrickson, W. A. *Langmuir* **1992**, 8, 921.
- (23) Sharma, A.; Reiter, G. *J. Colloid Interface Sci.* **1996**, 178, 383.
- (24) Register, R. A.; Prud'homme, R. K. In *Ionomers: Synthesis, Structure, Properties and Applications*; Tant, M. R., Mauritz, K. A., Wilkes, G. L., Eds.; Blackie Academic and Prof. Publ.: London, 1997; Chapter 5.
- (25) Yerushaimi-Rozen, R.; Klein, J.; Fetters, L. *Science* **1994**, 263, 793.
- (26) Yerushaimi-Rozen, R.; Klein, J. *Langmuir* **1995**, 11, 2806.
- (27) Reiter, G.; Auroy, P.; Auvray, L. *Macromolecules* **1996**, 29, 2150.
- (28) Chakrabarty, K.; Shao, L.-Y.; Weiss, R. A. In *Ionomers: Synthesis, Structure, Properties and Applications*; Tant, M. R., Mauritz, K. A., Wilkes, G. L., Eds.; Blackie Academic and Prof. Publ.: London, 1997; Chapter 4.
- (29) Feng, Y.; Schmidt, A.; Weiss, R. A. *Macromolecules* **1996**, 29, 3909.
- (30) Feng, Y. Ph.D. Thesis, University of Connecticut, 1995.
- (31) The reference to commercial equipment does not imply its recommendation or endorsement by the National Institute of Standards and Technology. According to ISO 31-8, the term molecular weight has been replaced by "relative molecular mass"  $M_r$ . The older, more conventional notation for number

- average ( $M_n$ ) and weight average ( $M_w$ ) molecular weights is utilized in the present paper.
- (32) Makowski, H. S.; Lundberg, R. D.; Singhal, G. H. US Patent, 3,870,841, 1975.
- (33) Russell, T. P.; Karim, A.; Mansour, A.; Felcher, G. P. *Macromolecules* **1988**, *21*, 1890.
- (34) Russell, T. P. *Mater. Sci. Rep.* **1990**, *5*, 171.
- (35) Patil, R.; Kim, S.-J.; Smith, E.; Reneker, D. H.; Weisenhorn, A. L. *Polymer Commun.* **1990**, *31*, 455.
- (36) Karim, A.; Tsukruk, V. V.; Douglas, J. F.; Satija, S. K.; Fetters, L. J.; Reneker, D. H.; Foster, M. D. *J. Phys. II (Fr.)*, **1995**, *5*, 1441.
- (37) Faldi, A.; Composto, R. J.; Winey, K. I. *Langmuir* **1995**, *11*, 4855.
- (38) Weiss, R. A., *J. Polym. Sci.: Polym. Phys. Ed.* **1982**, *20*, 65.
- (39) Eisenberg, A., Ed., *In Ions in Polymers*; Advances in Chemistry 187; American Chemical Society: Washington DC, 1980.
- (40) Noshay, A.; Robeson, L. M. *J. Appl. Polym. Sci.* **1976**, *20*, 1885.
- (41) Eisenberg, A.; Yeo, S. C. *J. Appl. Polym. Sci.* **1977**, *21*, 875.
- (42) Weiss, R. A.; Lundberg, R. D.; Werner, A. *J. Polym. Sci.: Polym. Chem. Ed.*, **1980**, *18*, 3427.
- (43) Siadat, B.; Oster, B.; Lenz, R. W. *J. Appl. Polym. Sci.* **1981**, *26*, 1027.
- (44) Weiss, R. A.; Turner, S. R.; Lundberg, R. D. *J. Polym. Sci.: Polym. Phys. Ed.* **1985**, *23*, 525.
- (45) Ferry, J. D. *Viscoelastic Properties of Polymers*, 3rd ed.; Wiley: New York, 1980.
- (46) Weiss, R. A.; Fitzgerald, J. J.; Kim, D. *Macromolecules* **1991**, *24*, 1064, 1071.

MA9706541